EARTHQUAKE ENGINEERING AND STRUCTURAL DYNAMICS
Earthquake Engng Struct. Dyn. (2011)
Published online in Wiley Online Library (wileyonlinelibrary.com). DOI: 10.1002/eqe.1096

A new indicator of elastic spectral shape for the reliable selection of ground motion records

Mehdi Mousavi[1], Mohsen Ghafory-Ashtiany[1] and Alireza Azarbakht[2,*,†]

[1]*International Institute of Earthquake Engineering and Seismology (IIEES), Tehran, Iran*
[2]*Department of Civil Engineering, Faculty of Engineering, Arak University, Iran*

SUMMARY

How to select a limited number of ground motion records (GMRs) is an important challenge for the non-linear analysis of structures. Since epsilon (ε_{Sa}) is an indicator of spectral shape, which has a significant correlation with the non-linear response of a structure, the selection of GMRs based on the hazard-related target ε_{Sa} is a reasonable approach. In this paper, an alternative indicator of spectral shape is proposed, which results in a more reliable prediction of the non-linear response for the structures with the natural period of 0.25 to 3.0 s. This new parameter, named eta (η), is a linear combination of ε_{Sa} and the peak ground velocity epsilon (ε_{PGV}). It is shown that η, as a non-linear response predictor, is remarkably more efficient than the well-known and convenient parameter ε_{Sa}. The influence of η-filtration in the collapse analysis of an eight-story reinforced concrete structure with special moment-resisting frames was studied. Statistical analysis of the results confirmed that the difference between ε-filtration and η-filtration can be very significant at some hazard levels. In the case of this structure, the resulting annual frequency of collapse was found to be lower in the case of η-based record selection, in comparison with the ε-based record-selection approach. Copyright © 2011 John Wiley & Sons, Ltd.

Received 19 April 2010; Revised 3 November 2010; Accepted 19 November 2010

KEY WORDS: ground motion record; spectral shape; collapse capacity assessment; epsilon; eta; hazard level

1. INTRODUCTION AND GOALS OF THE STUDY

One of the challenges in assessing structural collapse performance is the appropriate selection of ground motion records (GMRs) for use in non-linear dynamic collapse simulation. The GMR selection issue was studied from different viewpoints in a few recent researches [1, 2].

The current best record-selection practice (e.g. [3]) recommends using seven or fewer records, which represent the magnitude and the distance identified by probabilistic seismic hazard analysis (PSHA) disaggregation [4]. These records are then scaled (if necessary), in one manner or another, to match the level of the uniform hazard spectrum (UHS). For a given ground motion hazard level (e.g. a 2% chance of exceedance in 50 years), it has been shown that the shape of the UHS can be quite different from the shape of the expected response spectrum of a real GMR having an equally high spectral amplitude at a particular period [5, 6]. For this reason, the current code-based practice is usually conservatively biased for structural collapse assessment [6]. Also, it is shown that there is not enough evidence to prove the hypothesis of influence of using the magnitude and distance on the structural non-linear response [7]. Spectral shape characteristics are especially important

*Correspondence to: Alireza Azarbakht, Department of Civil Engineering, Faculty of Engineering, Arak University, P.O. Box 38156-88359, Iran.
†E-mail: a-azarbakht@araku.ac.ir

for structural collapse assessment because it is at high amplitudes that these differences are the most significant [8, 9]. One approach that can be used to take into account the spectral shape in structural analysis is to select and scale GMRs by an intensity measure (IM) other than $S_a(T_1)$, which accounts for the spectral shape in either an implicit or an explicit manner. Possible IMs include the inelastic spectral displacement [10], or the spectral value averaged over a period range [6]. However, since the seismic hazard parameters have not yet been developed for these IMs, the preferred approach is to use the convenient $S_a(T_1)$.

It is quite well known that the response spectra epsilon (ε) is an indicator of the elastic spectral shape of GMRs [6]. The parameter ε is a measure of the difference between the spectral acceleration of a record and the mean value of the spectral acceleration, obtained from a ground-motion prediction equation at a given period. It is noteworthy that the parameter ε has a seismological origin. The three parameters that can vary for a given site and a given fault are magnitude (M_w), distance (R), and ε [11]. The relative contribution of these parameters to the rate of exceedance of a given ground motion IM can be calculated by the application of the seismic disaggregation procedure [4, 12]. The combination of M_w, R and ε, which provides the largest contribution to the desired hazard, is interpreted as the *earthquake scenario*. Therefore, the most direct approach that can be used to account for the spectral shape in structural analysis is to select GMRs that have M_w, R and ε values that match the target values obtained from the corresponding disaggregation analysis.

The parameter ε is not a perfect indicator of spectral shape due to the random nature of ground motion records. The ε values of GMRs and the associated non-linear response of a given structure are in partial correlation. The ability of ε to predict the non-linear response of a given structure depends on the strength of this correlation.

The objective of this study is to investigate the robustness of ε as a non-linear response predictor, and also to establish a more reliable indicator of spectral shape which could lead to a better prediction of non-linear response. The main idea belonging to this goal is the incorporation of the time-domain IMs (i.e. PGA, PGV and PGD) with the frequency-domain IMs (i.e. the spectral values) in order to create a more reliable indicator of the elastic spectral shape.

Even if the parameter ε is usually related to the acceleration response spectra, it can also be extended to each arbitrarily selected IM, as expressed in Equation (1):

$$\varepsilon_{\mathrm{IM}} = \frac{\ln \overline{\mathrm{IM}} - \ln \mathrm{IM}}{\sigma_{\ln \mathrm{IM}}} \tag{1}$$

where $\overline{\mathrm{IM}}$ and IM are, respectively, the observed IM and the attenuation-related IM, and $\sigma_{\ln \mathrm{IM}}$ indicates the anticipated standard deviation for the predicted IM. The aim is to find a new indicator, hereinafter named 'eta' (η), as a function of the different epsilons, which would result in a better indication of the spectral shape.

If a combination of different epsilons is to be used for record selection, the choice of the target value of the included epsilons is a practical challenge. As mentioned above, a standard hazard disaggregation analysis can provide only the target ε, whereas the other target epsilons are undetermined. Assuming similar values for these epsilons might be challengeable since these different epsilons might not be equal at different hazard levels. All of these aspects are discussed in this paper.

2. EPSILON; A PREDICTOR OF NON-LINEAR RESPONSE

The parameter ε is an indicator of the spectral shape, as mentioned in the previous section, and as a result, the collapse capacity of a given structure can be influenced by this. In order to investigate the effect of ε on the non-linear response of a structure, a set of non-linear single-degree-of-freedom (SDOF) systems, as well as an appropriate bin of GMRs, was considered. A period range of 0.1–2.0 s, as well as a ductility range of 2 to 12, was used for the SDOF systems. The collapse capacity values were calculated using incremental dynamic analysis (IDA), and a precise trace

DOI: 10.1002/eqe

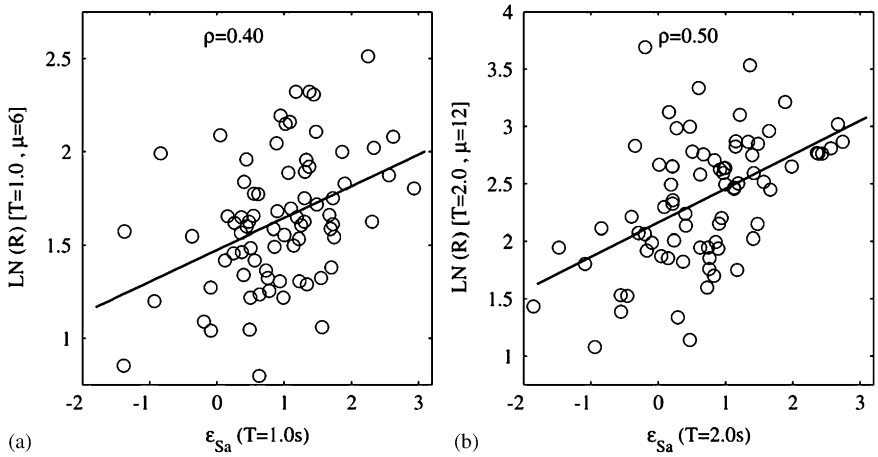

Figure 1. The correlation between the parameter ε_{Sa} and the collapse capacity values: (a) $T=1.0$ s, $\mu=6$ and (b) $T=2.0$, $\mu=12$.

of the collapse capacity point was performed using the Hunt and Fill algorithm [13]. The bin of applied GMRs includes 78 records, with a magnitude range of 6.5–7.8. These records were obtained from the PEER web site [14]. The selection criteria and the other information can be found in [15]. More details of structural systems, collapse assessment procedure and GMRs bin are referred in the Appendix A.

Figure 1 shows the correlation between the parameter ε and the collapse capacity values for two SDOF systems with periods of 1.0 and 2.0 s, and ductility values equal to 6 and 12. The epsilon values were determined based on the Campbell and Bozorgnia attenuation relationship [16].

The correlation shown in Figure 1 confirms the influence of the parameter ε on the non-linear response. Owing to this correlation, it is anticipated that the selection of GMRs based on ε-filtration results in a reduction in the potential bias in the prediction of the structural non-linear response. It is clear that the amount by which the potential bias can be reduced strongly depends on the size of the correlation between the non-linear response and the parameterε. For example, due to the higher correlation in the case of the more ductile system, as shown in Figure 1, the epsilon is more efficient for systems with higher ductility compared with other less ductile SDOF systems. The correlation coefficient (ρ) between two random variables X and Y with the expected values μ_X and μ_Y and standard deviations σ_X and σ_Y was defined as the covariance normalized by the product of their standard deviations, as written in Equation (2).

$$\rho=\frac{\mathrm{cov}(X,Y)}{\sigma_X\sigma_Y}=\frac{E((X-\mu_X)(Y-\mu_Y))}{\sigma_X\sigma_Y} \tag{2}$$

The greater influence of epsilon on ductile structures has also been inferred in the other studies [8]. The above analysis for all of the considered SDOF systems showed that the average correlation coefficient is just 0.43 (0.31, 0.41, 0.42, 0.45, 0.48 and 0.51 for different ductility values). It is reasonable to take this correlation coefficient as an index of efficiency of the parameter ε_{Sa} for reducing the potential bias in the non-linear response.

The potential of other IMs, such as epsilons (ε_{IM}), as response predictors can also be investigated. For example, Figure 2 shows the collapse capacity values of an SDOF system versus ε_{PGA} andε_{PGV}. Each of the individual parameters ε_{PGA} and ε_{PGV} can be treated as a response predictor, although they show a lower efficiency, as shown in Figure 2, in comparison with ε_{Sa}.

The main contribution of this study is that a more robust predictor of non-linear response has been obtained by considering the parameter η as a linear combination of different epsilons. This hypothesis is studied in the following section.

DOI: 10.1002/eqe

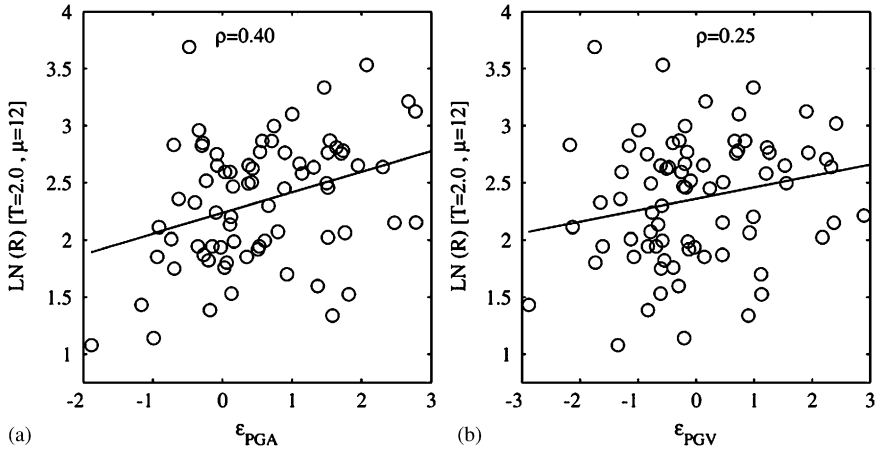

Figure 2. The correlation between the time-domain epsilon values and the collapse capacity values: (a) ε_{PGA} and (b) ε_{PGV}.

3. ETA; A MORE ROBUST PREDICTOR OF NON-LINEAR RESPONSE

Each of the IM epsilons can reflect a part of information hidden in a given GMR. Here, it is shown that a combination of IM epsilons can result in a more robust prediction of the structural response.

Again, let us assume an SDOF system with a period of 2.0 s and ductility equal to 12. A linear trend, as expected, exists between ε_{Sa} and the non-linear response as shown in Figure 3(a). The correlation coefficient between these variables was determined to be equal to 0.50. Now consider the parameter η as a linear combination of ε_{Sa}, ε_{PGA}, ε_{PGV} and ε_{PGD} as written in Equation (3):

$$\eta = \varepsilon_{Sa} + c_1\varepsilon_{PGA} + c_2\varepsilon_{PGV} + c_3\varepsilon_{PGD} \tag{3}$$

The objective is to find the best values for the constant coefficients (c_1, c_2 and c_3), which result in the maximum correlation between η and the non-linear response. By application of the Genetic Algorithm (GA) [17], as a powerful tool for optimization, the optimum constant coefficients were determined to be equal to:

$$c_1 = 0.50, \quad c_2 = -0.74, \quad c_3 = -0.42$$

The achieved correlation coefficient is 0.75, and is significantly greater than the previously obtained value, as shown in Figure 3(b). It is thus reasonable to claim that the potential of η is greater than ε_{Sa} to predict the non-linear response.

Equation (3) was based on just one particular case, and hence it does not represent all of the investigated SDOF systems. A regression analysis for the response of all of the SDOF systems is needed in order to develop a general response predictor. Since the non-linear response of each SDOF system is related to its characteristics (period and ductility), it is necessary to involve the period and the ductility values in the regression analysis. However, since the major purpose of a response predictor is to predict how any record provides a high response or a low response, the dependency of the response predictor on the structural characteristics can be removed with the normalization of each SDOF response to the standard form with a zero mean and unit variance. As illustrated in the Appendix A, the goodness of the normal distribution to the logarithm values of the response is confirmed, so that such a normalization is completely reasonable.

After normalization of all of the SDOF response values, a vector of size 6552 (84×78) was obtained. Corresponding to this vector, a 6552×4 matrix, including four epsilon values for each record and each SDOF system, was considered. Similar to the above approach, the response predictor (η) can be defined. For sensitivity analysis, too, different combinations of epsilons are involved in the regression analysis, and the results are summarized in Table I.

DOI: 10.1002/eqe

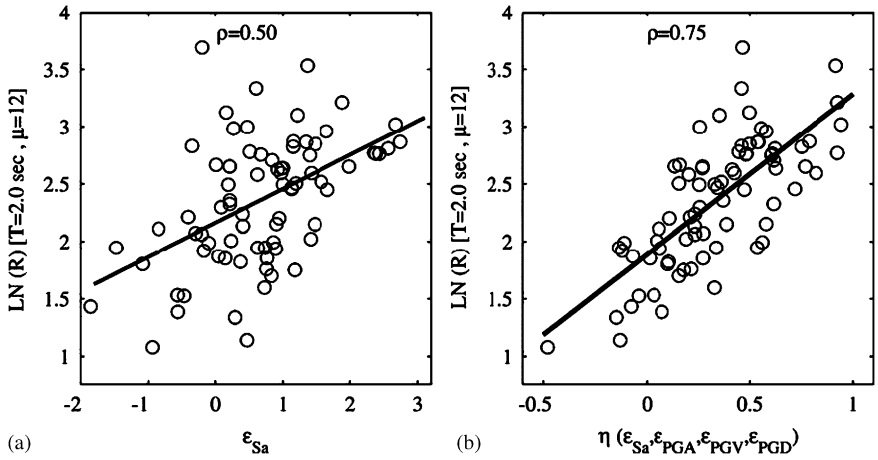

Figure 3. The correlation between the response predictors and the collapse capacity: (a) ε_{Sa} as a response predictor and (b) η as a response predictor.

Table I. Determination of the coefficients for η for different linear combinations of ε.

No.	ε_{Sa}	ε_{PGA}	ε_{PGV}	ε_{PGD}	ρ
1	1	—	—	—	0.43
2	—	1	—	—	0.18
3	—	—	1	—	0.08
4	—	—	—	1	0.13
5	1	−0.373	—	—	0.47
6	1	—	−0.823	—	0.64
7	1	—	—	−0.676	0.54
8	1	0.123	−0.958	—	0.65
9	1	−0.289	—	−0.540	0.56
10	1	0.186	−1.016	0.057	0.65

Table II. Median values of b and ρ, versus the bootstrapped standard error and the 95% confidence interval.

	Median	Standard error	95% confidence interval
b	0.823	0.012	[0.791, 0.845]
ρ	0.65	0.01	[0.63, 0.66]

The last case, which involves all of the epsilons, provides, as shown in Table I, the most efficient response predictor, with $\rho=0.65$. However, it can be seen that the efficiency of the dual combination of ε_{Sa} and ε_{PGV} (the sixth item in Table I) is approximately equal to that of the last combination. Thus, a simple definition of the parameter η can be introduced as:

$$\eta=\varepsilon_{Sa}-b\varepsilon_{PGV}, \quad b=0.823 \tag{4}$$

The bootstrap method was used to analyze how significant the resulted regression coefficient is [18]. The application of the bootstrap method involves sampling with replacement from the 6552 (84×78) data-points to generate an arbitrary number of alternate data-points, and apply GA to find the optimum value of b so that a maximum value of ρ is obtained in each case. From such samples of estimates, it is easy to calculate the standard error and the confidence intervals for both values of b and ρ. The standard error and the 95% bootstrap confidence interval for b, and for ρ, are shown in Table II.

DOI: 10.1002/eqe

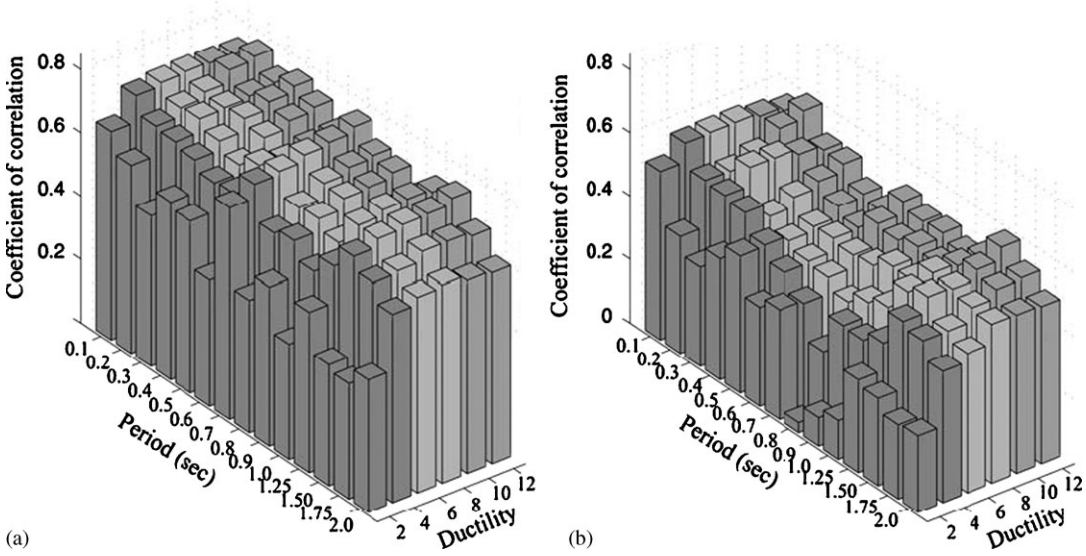

Figure 4. Comparison of the efficiency of η and $\varepsilon_{\mathrm{Sa}}$ as response predictors: (a) correlation of the response and η (b) correlation of the response and $\varepsilon_{\mathrm{Sa}}$.

It is clear that the used data-points provide a relatively accurate model for the parameter η, since the median values of b and ρ show only a small dispersion.

As an interesting result in Table I, $\varepsilon_{\mathrm{PGV}}$ is a poor predictor of non-linear response when it used alone, but when it is combined with $\varepsilon_{\mathrm{Sa}}$ the resulting combination provides a good predictor of the non-linear response. It is worth emphasizing that the epsilons should, in this case, be combined with opposite signs in order to construct the best predictor of the non-linear response. Recalling that $\varepsilon_{\mathrm{IM}}$ is related to the logarithm of IM for a given GMR, this phenomenon can be interpreted as the parameter η is related to the ratio $S_a(T_1)/\mathrm{PGV}$. Consequently, this ratio can be accounted as an indicator of elastic spectral shape, which is in agreement with the previous findings that express that the PGA/PGV ratio is related to the frequency content of GMRs [19, 20]. As a result, for two GMRs with similar $\varepsilon_{\mathrm{Sa}}$, the record with the higher $\varepsilon_{\mathrm{PGV}}$ is expected to provide lower collapse capacity and vice versa.

Figures 4(a) and (b) show, respectively, the correlation coefficient between the parameters η and $\varepsilon_{\mathrm{Sa}}$ and the non-linear response for all of the investigated SDOF systems. The parameter η is a more robust predictor of response as shown in Figure 4, with an average of a 50% improvement in the correlation coefficient.

The improved efficiency of η as a response predictor may be due to the fact that η is a better indicator of the spectral shape than $\varepsilon_{\mathrm{Sa}}$. This hypothesis is demonstrated in Figure 5. The GMRs were sorted based on the $\varepsilon_{\mathrm{Sa}}$ value and also based on η, and then two higher and lower subsets with N elements were selected from each sorted list. The mean of the response spectra of both subsets were then plotted, so that the left-hand figures are based on $\varepsilon_{\mathrm{Sa}}$ sorting and the right-hand figures are based on η-based sorting. Two subsets with size 8, as shown in Figure 5(a), result in different spectral shapes. This finding is similar to the results obtained in other studies (i.e. [6]). The procedure is repeated for η filtration in Figure 5(b). The difference between two resulted spectra is more significant for the η-filtration case in comparison with the $\varepsilon_{\mathrm{Sa}}$-filtration approach. This analysis was repeated for a selection of 16 records, and the corresponding results are shown in Figures 5(c) and (d), for each of the filtration approaches. This case fully confirms the better ability of η to make a distinction between records with different spectral shapes.

The η values classify the response spectrum in both the higher and lower periods, as shown in Figure 5, although this approach is based on the analysis of the non-linear response of the investigated SDOF systems. The η-filtration approach thus provides reliable GMRs even in the case of MDOF structures with considerable effects of higher modes.

DOI: 10.1002/eqe

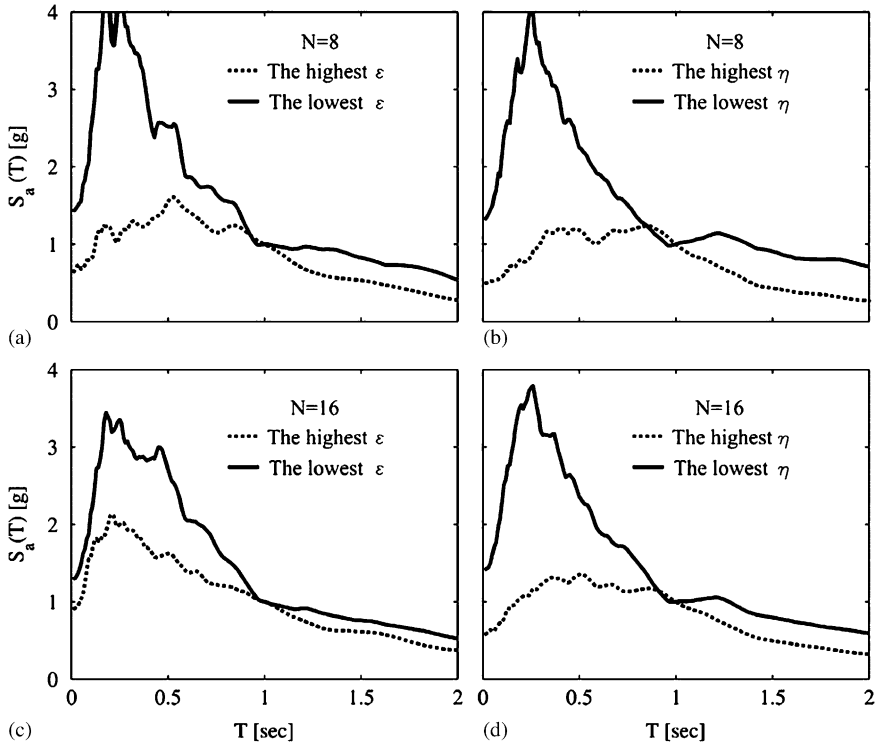

Figure 5. Comparison of η and ε_{Sa} as indicators of spectral shape (a), (b) selection of 8 ground motions with highest/lowest values of η and ε_{Sa} and (c), (d) selection of 16 ground motions with highest/lowest values of η and ε_{Sa}.

4. DETERMINATION OF THE TARGET ETA FOR DIFFERENT HAZARD LEVELS

A practical challenge faced when using η for record selection is the choice of target epsilons. Ground-motion prediction models predict the probability distributions of IMs for a specified earthquake event. These models provide only marginal distributions, but they do not specify correlations among differing IMs. On the other hand, standard hazard disaggregation analysis only provides the target ε_{Sa}, but the target ε_{PGV} is still undetermined. Assuming equal values for epsilons may be challengeable since equal epsilons may not necessarily correspond to a particular hazard level. The correlation between ε_{PGV} and ε_{Sa} in different period ranges is studied in this section, and linear regression is implemented in order to develop an analytical equation for the evaluation of ε_{PGV} for a given ε_{Sa}.

The results presented in this section were derived empirically from a strong ground motion records (SGMRs) data set based on worldwide recordings of shallow crustal earthquakes. This set, which was used by Baker and Cornell [21] to analyze the correlation of response spectral values, includes 267 pairs of horizontal GMRs with magnitudes greater than 5.5 and source-to-site distances of less than 100 km. The other selection criteria, as well as the detailed documentation about this set, are given in [5].

Figure 6(a) shows the correlation coefficient between ε_{PGV} and ε_{Sa} for different periods. The parameter ε_{PGV} is not enough correlated, as shown in Figure 6(a), with ε_{Sa} in lower periods; hence, the periods less than 0.25 s are neglected from the correlation analysis, as a rational judgment.

The correlation between ε_{PGV} and ε_{Sa} can be represented by the following model:

$$\varepsilon_{PGV} = c_0 + c_1 \varepsilon_{Sa} \tag{5}$$

Figure 6(b) shows the correlation analysis results for periods 0.5, 1.0 and 2.0 s. Because the three fitted lines have slopes that are roughly similar, it seems that there is not any meaningful difference

DOI: 10.1002/eqe

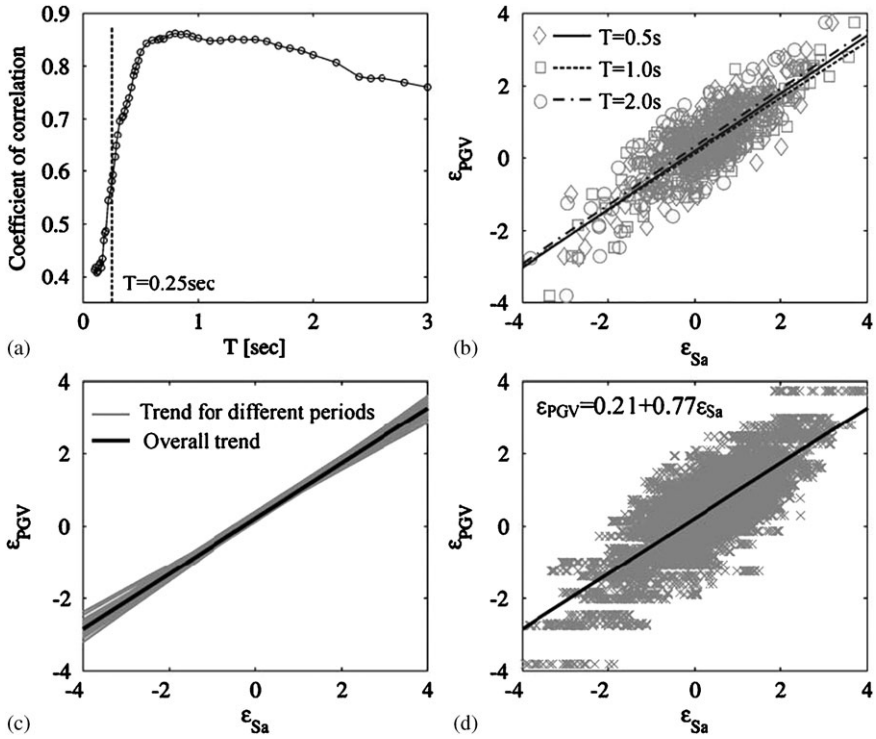

Figure 6. Analysis of covariance of ε_{PGV} and ε_{Sa}: (a) the correlation coefficient versus period; (b) the fitted lines for three different periods; (c) the regression analysis for different periods; and (d) the final regression analysis for total periods.

between the different fitted lines. This analysis is repeated for all period with the range of 0.25–3.0 s in Figure 6(c). The evidence of dependency of regression coefficients to the period was tested by implementing the analysis of covariance, as a well-known statistical tool. The F statistic was employed to test the null hypothesis (NH) that the regression models are similar, and rejection of the NH is taken to indicate the dependency of fitted lines to period. The risk of type I error (the probability of rejecting the NH when it is true) is given by α, which was taken to be 0.05, and the smallest fixed level at which this occurs is p, the observed level of significance. If $p<\alpha$, then the NH is rejected at the 0.05 significance level. With a p-value of 0.50, there is not enough evidence to reject the NH (see details of analysis of covariance in [22]). Therefore, it is sensible to employ all of periods in order to develop a unique equation for prediction of ε_{PGV} from ε_{Sa}. Figure 6(d) shows ε_{PGV} versus ε_{Sa} for the considered data-points. The overall linear regression analysis results in:

$$c_0 = 0.24 \ [0.23\text{–}0.26], \quad c_1 = 0.72 \ [0.70\text{–}0.73]$$

The bracketed values indicate 95% confidence intervals, which are calculated from standard statistics [22]. The correlation coefficient between ε_{Sa} and ε_{PGV}, and the associated 95% confidence interval, are estimated as:

$$\rho = 0.80 \ [0.79\text{–}0.82]$$

A direct method to account for the target η in structural collapse assessment is to determine the expected ε_{PGV} value from Equation (5) for any considered hazard level, then to calculate the target η from Equation (4) and finally, to select the ground motions that are consistent with the target η. For the purposes of simplicity, Equation (4) can be revised to normalize the target η values to the target ε_{Sa} values, as described as follows:

$$\eta = k_0 + k_1(\varepsilon_{Sa} - b\varepsilon_{PGV}) \tag{6}$$

DOI: 10.1002/eqe

It is clear that, due to the linear correlation between the η values and the structural response, this adjustment is permissible. Now, by substituting ε_{PGV} from Equation (5) into Equation (6), and considering the target η to be equal to the target ε_{Sa}, k_0, k_1 can be determined as:

$$k_0 = \frac{bc_0}{1-bc_1} = 0.472, \quad k_1 = \frac{1}{1-bc_1} = 2.730$$

By replacing the above constant values in Equation (6), the final form of η is obtained as:

$$\eta = 0.472 + 2.730\varepsilon_{Sa} - 2.247\varepsilon_{PGV} \tag{7}$$

The target η value can now be considered to be equal to the target ε_{Sa} that is achievable from the disaggregation analysis. It should be noted that the application domain of the η-filtration approach is limited to periods from 0.25 to 3.0 s. In the following section, an η-based selection of ground motion records is presented for the collapse simulation of an MDOF structure.

5. EXAMPLE: COLLAPSE CAPACITY ASSESSMENT OF AN MDOF STRUCTURE

In this section, the seismic collapse capacity of an MDOF test structure based on an η-based record selection is discussed. The considered structure is an eight-story reinforced concrete building with special moment-resisting frames. The building is 36.5×36.5 m in plan, uses a 3-bay perimeter frame system with a spacing of 6.1 m, and has a fundamental period (T_1) of 1.71 s. This building is ID 1011 from [15]. The mathematical model of this structure that was created [15] within the OpenSees program [23] was used in this section. It was assumed that this structure is located at an idealized site where the ground motion hazard is dominated by a single characteristic event with a return period of 200 years, $M_w = 7.2$, $R = 11.0$ km and Vs_30 = 360 m/s.

From the basic probability theory, the annual frequency of exceedance (υ) for $\ln S_a(T) > x$ can be written as:

$$\upsilon[\ln S_a(T) > x] = \upsilon_0 P[\ln S_a(T) > x | \mathrm{Mw}, R] \tag{8}$$

where υ_0 is the annual frequency of the earthquake, which is in this case equal to $\frac{1}{200}$. First, x is taken equal to the value predicted by the attenuation relation ($\overline{\ln S_a(T)}$), which corresponds to the zero epsilon value:

$$\upsilon[\ln S_a(T) > \overline{\ln S_a(T)}] = \upsilon_0 P[\ln S_a(T) > \overline{\ln S_a(T)} | \mathrm{Mw}, R] = \tfrac{1}{200} \times 0.50$$

Assuming a normal distribution for $\ln S_a(T)$, Equation (8) can be re-written for $\varepsilon_{Sa} = 0.80$ as:

$$\upsilon[\ln S_a(T) > \overline{\ln S_a(T)} + 0.80\sigma] = \upsilon_0 P[\ln S_a(T) > \overline{\ln S_a(T)} + 0.80\sigma | \mathrm{Mw}, R] = \frac{1}{200} \times 0.21$$

Considering that $\frac{1}{200} \times 0.21 = \frac{1}{475} \times 0.50$, it is a reasonable to infer that $\varepsilon_{Sa} = 0.80$ is equivalent to an event with a return period of 475 years. Using this approach, the target epsilons for different hazard levels are given in Table III.

The GMRs bin that was introduced previously is appropriate for this site. The magnitude–distance distribution of this bin, which is shown in Appendix A, confirms its consistency with

Table III. The target parameters for different hazard levels.

Return period (year)	Probability in 50 years (%)	Target epsilon
125	33	−0.80
200	22	0.00
475	10	+0.80
2475	2	+1.75

DOI: 10.1002/eqe

Table IV. Mean collapse capacities of the structure based on $\varepsilon_{\mathrm{Sa}}$ and η-filtration.

Return period (year)	$\varepsilon_{\mathrm{Sa}}$-based, $S_a(T=1.71\,\mathrm{s})$	η-based, $S_a(T=1.71\,\mathrm{s})$
125	0.53	0.57
200	0.56	0.69
475	0.76	0.84
2475	0.97	0.99

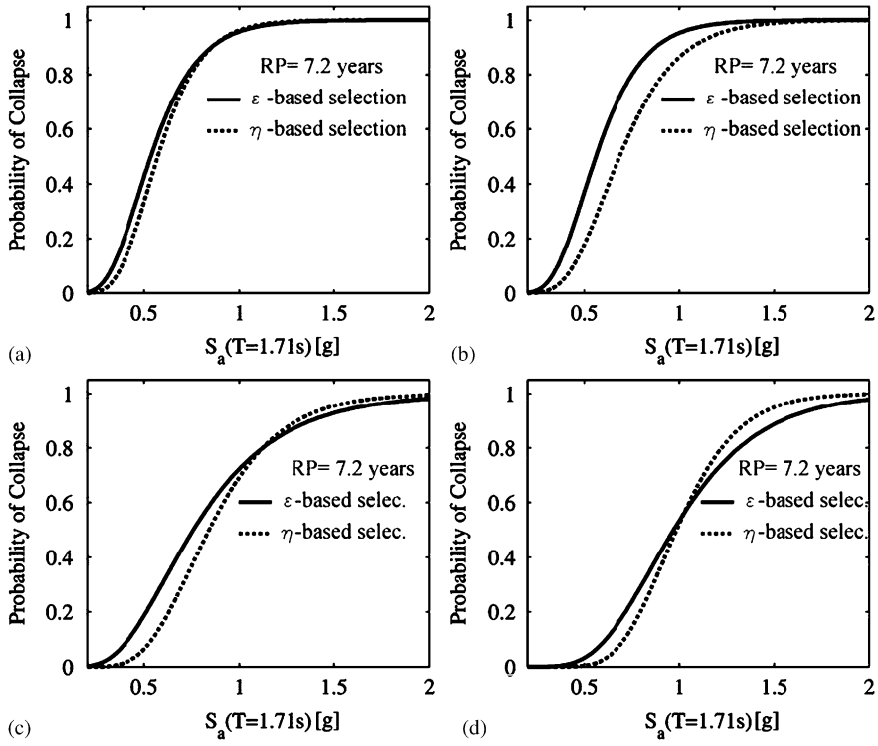

Figure 7. The fragility curves for different hazard levels: (a) a return period of 125 years; (b) a return period of 200 years; (c) a return period of 475 years; and (d) a return period of 2475 years.

the assumed earthquake scenario. For each hazard level, 20 GMRs were selected using both η-filtration and $\varepsilon_{\mathrm{Sa}}$-filtration procedures. The mean collapse capacity of the structure for each of the ground motion sets was calculated, and the results are shown in Table IV. It can be seen that the two different filtration approaches result in two distinct mean collapse capacities for some of the considered hazard levels. The resulting fragility curves for different hazard levels are shown in Figure 7, where the differences between the $\varepsilon_{\mathrm{Sa}}$ and η filtrations are, in the case of some of the epsilons, significant, whereas in the case of the remaining epsilons they are not significant.

In order to study further the influence of η filtration, the ground motion selection was performed for a relatively wide range of hazard levels. The results are shown in Figure 8(a), compared with the results obtained by $\varepsilon_{\mathrm{Sa}}$ filtration. A standard hypothesis test [22] was implemented for each discrete $\varepsilon_{\mathrm{Sa}}$ in order to determine whether or not this difference is meaningful. The NH is the equality of the two means. Figure 8(b) shows the resulting p-value for each $\varepsilon_{\mathrm{Sa}}$ value. By assuming a common significant level (i.e. 0.05), as shown in Figure 8(b), the NH can be rejected for $\varepsilon_{\mathrm{Sa}}=0, 0.25, 0.5$. It can therefore be concluded that a record selection based on η filtration may, at some hazard levels, lead to quite different results to those obtained by convenient $\varepsilon_{\mathrm{Sa}}$ filtration.

For further investigation, the mean annual frequency (MAF) of collapse was computed based on each of the filtration approaches. Figure 9(a) shows the hazard curve for the assumed site. The MAF of collapse due to $S_a(T=1.71\,\mathrm{s})=x$ is shown in Figure 9(b), for both record-selection

DOI: 10.1002/eqe

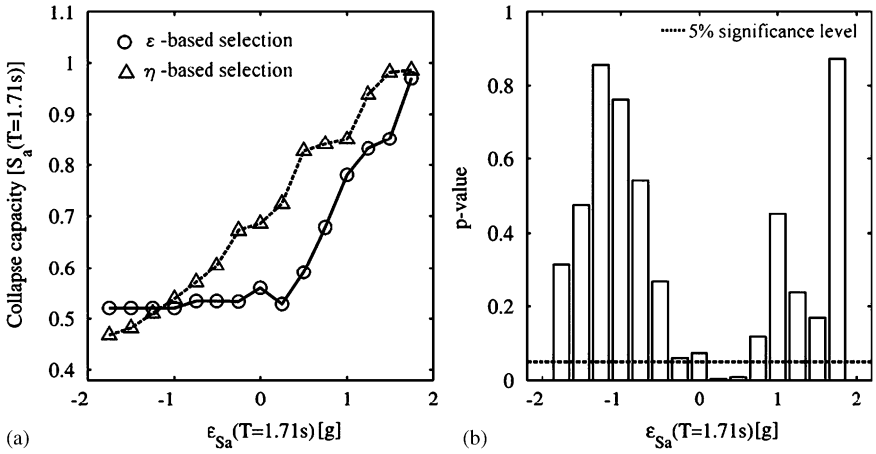

Figure 8. Mean collapse capacity of the MDOF structure based on $\varepsilon_{\mathrm{Sa}}$ and η filtration: (a) the difference between the two filtration approaches at difference levels of epsilon and (b) the results of the statistical hypothesis test for the equality of collapse capacity based on the two filtration approaches.

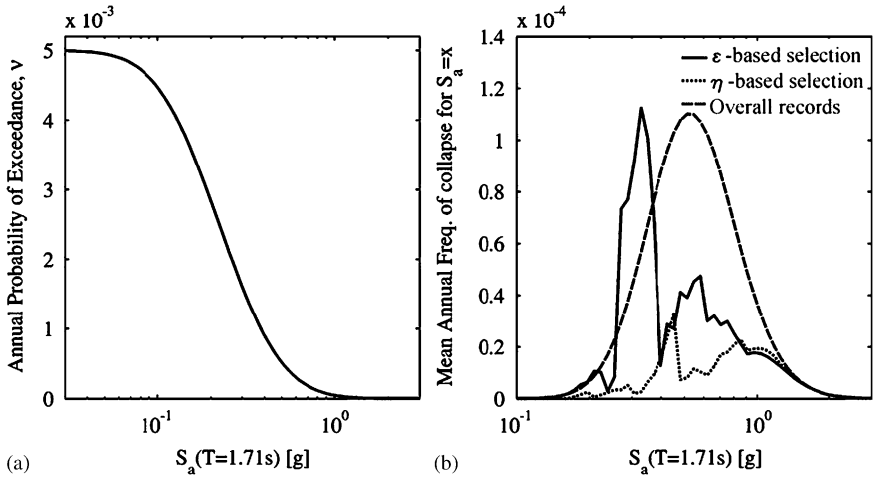

Figure 9. The effect of different filtration approaches in the MAF analysis: (a) the hazard curve and (b) the MAF of collapse due to $S_a(T=1.71\,\mathrm{s})=x$.

methods. The MAF of collapse is also shown in Figure 9(b) for the case when all the records were used (without any filtration). The MAF of collapse is less for $\varepsilon_{\mathrm{Sa}}$-filtration in comparison with the no-filtration approach, which has also been addressed by other studies (e.g. [6]). Also this figure shows that the MAF of collapse for η-filtration is remarkably lower than that for the $\varepsilon_{\mathrm{Sa}}$-filtration. The absolute value of MAF, calculated by integrating MAF over S_a, was 6.4×10^{-5}, 3.6×10^{-5} and 1.8×10^{-5} for the no-filtration, $\varepsilon_{\mathrm{Sa}}$-filtration and η-filtration approaches, respectively.

It is worth emphasizing that the greater reliability of the η approach for the selection of records was inferred due to the better correlation between this parameter and the structural non-linear response, comparing with $\varepsilon_{\mathrm{Sa}}$ (see Figure 4), and also due to the better indication of the elastic spectral shape as seen in Figure 5. Stochastic simulation of GMRs can be applied as a practical approach to explicitly verify the results (see the fundamental aspects of stochastic record simulation in [24]). However, as mentioned by Tothong [10], the correlation of response spectral values for simulated records differs from that of those corresponding to recorded far-field GMRs. The correlation of response spectra for a particular period among the neighboring period values in recorded GMRs decreases gradually, so that this trend is quite different in simulated GMRs [10]. As a consequence, at a particular period neither $\varepsilon_{\mathrm{Sa}}$ nor η signify the trend of the spectral shape

DOI: 10.1002/eqe

for the simulated records. Therefore, an explicit verification of the efficiency of η is not feasible through common simulation approaches. Modification of this conceptual limitation of simulated records is open for future studies.

6. CONCLUSIONS

As a predictor of non-linear response, the parameter ε_{Sa} is an efficient parameter that can be used to reduce bias in the structural non-linear response. In order to improve the reliability of the record-selection procedure, a new parameter named eta (η) has been proposed as a linear combination of ε_{Sa} and ε_{PGV}. It was shown that the correlation between η and the non-linear response is about 50% better than the correlation between ε_{Sa} and the response. It has also been shown that the parameter η is a better indicator of spectral shape compared with the parameter ε_{Sa}. Based on the results of regression analysis, an equation has been proposed for the prediction of the target ε_{PGV} based on a given ε_{Sa}. The influence of the parameter η on the collapse capacity assessment of an 8-story reinforced concrete building with special moment-resisting frames was investigated. The results showed that, at some hazard levels, the difference in the collapse capacity of structure resulting from η and ε_{Sa} filtration is meaningful. Also, the absolute MAF of collapse for the η-filtration approach is remarkably lower than that corresponding to ε_{Sa}-filtration.

APPENDIX A

Figure A1 shows the magnitude–distance distribution as well as the response acceleration of the SGMRs that were used to investigate the influence of ε_{Sa} on non-linear response. These records' bin was also used to propose the parameter η as a response predictor (Equation (3)).

The seismic collapse capacity database was established for 84 SDOF systems with a period range of 0.1–2.0 s ($T = 0.1$, 0.2, 0.3, 0.4, 0.5, 0.6, 0.7, 0.8, 0.9, 1.0, 1.25, 1.5, 1.75 and 2.0), six ductility values ($\mu_f = 2$, 4, 6, 8, 10 and 12), and a mass proportional critical damping ratio equal to 5%. A tri-linear backbone curve model with zero hardening slope ($\alpha_s = 0$) and fixed capping ductility ($\mu_c = 0.9\mu_f$), as shown in Figure A2(a), was selected. $P-\Delta$ effects and cyclic deterioration were neglected, for the purpose of simplicity. Seismic collapse capacity analysis of 14×6 SDOF systems, for 78 records, was used to create a 84×78 matrix of the collapse capacity data for statistical analysis. $S_a(T, 5\%)$ was used as the IM for the seismic collapse capacity assessment. The collapse capacity tracing procedure is presented in Figure A2(a) for an arbitrarily selected SDOF

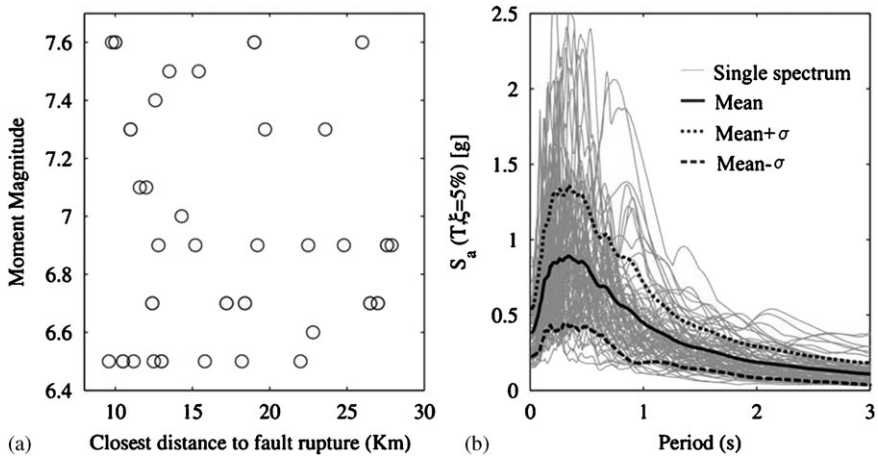

Figure A1. The SGMR's database: (a) the magnitude–distance distribution and (b) the acceleration response spectrum with 5% damping ratio.

DOI: 10.1002/eqe

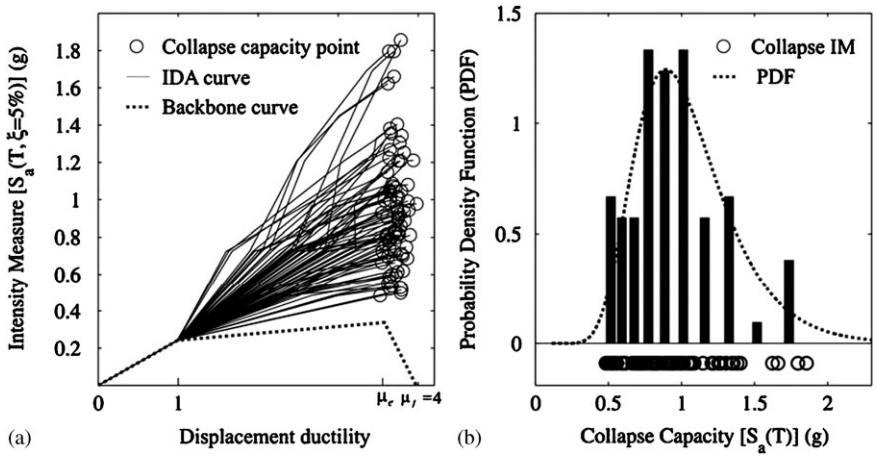

Figure A2. The seismic collapse capacity points in the IDA curves for an arbitrarily selected SDOF system and for the 78 GMRs where (a) an IM corresponding to a ductility equal to 4 is indicated, and (b) fitted by a log-normal distribution to the probability density function of the collapse capacity points.

system and for the 78 GMRs. The application of the Kolmogorov–Smirnov test [22] to the collapse capacity values of each SDOF system, as shown in Figure A2(b), confirmed the goodness of fitness of a normal distribution to the logarithm of the collapse capacity IM values. The minimum, average and maximum p-values for the considered SDOF systems in the Kolmogorov–Smirnov test are equal to, respectively, 0.17, 0.67 and 0.99.

ACKNOWLEDGEMENTS

The research conducted by the authors has been funded by the International Institute of Earthquake Engineering and Sesimology (IIEES) under Grant Number 7134. This support is gratefully acknowledged. Any opinions, findings, and conclusions or recommendations expressed in this material are those of the authors and do not necessarily reflect those of the funding body. The authors are also very grateful to both anonymous reviewers for their valuable comments.

REFERENCES

1. Katsanos E, Sextos A, Manolis G. Seismic ground motion selection and calibration for structural design: a review. *Soil Dynamics and Earthquake Engineering* 2010; **30**:157–169.
2. Beyer K, Bommer J. Selection and scaling of real accelerograms for bi-directional loading: a review of current practice and code provisions. *Journal of Earthquake Engineering* 2007; **11**(1):13–45.
3. ASCE7–05. Minimum design loads for buildings and other structures. *ASCE7–05*, American Society of Civil Engineers, Reston, VA, 2005.
4. Bazzurro P, Cornell CA. On disaggregation of seismic hazard. *Bulletin of the Seismological Society of America* 1999; **89**(2):501–520.
5. Baker JW. Vector-valued ground motion intensity measures for probabilistic seismic demand analysis. *Ph.D. Dissertation*, Department of Civil and Environmental Engineering, Stanford University, 2005.
6. Baker JW, Cornell CA. Spectral shape, epsilon and record selection. *Earthquake Engineering and Structural Dynamics* 2006; **34**(10):1193–1217.
7. Iervolino I, Cornell CA. Record selection for nonlinear seismic analysis of structures. *Earthquake Spectra* 2005; **21**(3):685–713.
8. Haselton CB, Baker JW, Liel AB, Deierlein GG. Accounting for ground motion spectral shape characteristics in structural collapse assessment through an adjustment for epsilon. *ASCE Journal of Structural Engineering*, DOI: 10.1061/(ASCE)ST.1943-541X.0000103.
9. Zareian F, Krawinkler H. Assessment of probability of collapse and design for collapse safety. *Earthquake Engineering and Structural Dynamics* 2007 **36**:1901–1914.
10. Tothong P. Probabilistic seismic demand analysis using advanced ground motion intensity measures, attenuation relationships, and near-fault effects. *Ph.D. Dissertation*, Department of Civil and Environmental Engineering, Stanford University, 2007.
11. Kramer SL. *Geotechnical Earthquake Engineering*. Prentice Hall: Upper Saddle River, NJ, 1996; 653.

DOI: 10.1002/eqe

12. McGuire RK. Probabilistic seismic hazard analysis and design earthquakes: closing the loop. *Bulletin of the Seismological Society of America* 1995; **85**:1257–1284.
13. Vamvatsikos D, Cornell CA. Incremental dynamic analysis. *Earthquake Engineering and Structural Dynamics* 2002; **31**(3):491–514.
14. PEER. Strong motion database. Available from: http://peer.Berkeley.edu/NGA.
15. Haselton CB, Deierlein GG. Assessing seismic collapse safety of modern reinforced concrete frame. *PEER Report 2007/08*, Pacific Engineering Research Center, University of California, Berkeley, CA, 2007.
16. Campbell KW, Bozorgnia Y. Campbell–Bozorgnia NGA ground motion relations for the geometric mean horizontal component of peak and spectral ground motion parameters. *PEER Report 2007/02*, Pacific Engineering Research Center, University of California, Berkeley, CA, 2007.
17. Goldberg DE. *Genetic Algorithms in Search, Optimization, and Machine Learning*. Addison-Wesley: Reading, MA, 1989.
18. Efron B, Tibshirani RJ. *An Introduction to the Bootstrap*. Chapman & Hall/CRC: New York, 1993.
19. Tso WK, Zhu TJ, Heidebrecht AC. Engineering application of ground motion A/V ratio. *Soil Dynamics and Earthquake Engineering* 1992; **11**:133–144.
20. Sawada T, Hirao K, Yamamoto H, Tsujihara O. Relation between maximum amplitude ratio and spectral parameters of earthquake ground motion. *Proceedings of 10th World Conference of Earthquake Engineering*, vol. 2, Madrid, Spain, 1992.
21. Baker JW, Cornell CA. Correlation of response spectral values for multicomponent ground motions. *Bulletin of the Seismological Society of America* 2006; **96**(1):215–227.
22. Hogg RV, Ledolter J. *Engineering Statistics*. MacMillan: New York, 1987.
23. McKenna F, Fenves GL, Jeremic B, Scott MH. Open system for earthquake simulations, 2000. Available from: http://opensees.berekely.edu.
24. Boore DM. Simulation of ground motion using the stochastic method. *Pure and Applied Geophysics* 2003; **160**(3):635–676.

DOI: 10.1002/eqe